Experimental measurement of cooling tower emissions using image processing of sensitive papers

J. Ruiz[a,*], M. Ballesta[a], A. Gil[c], A.S. Kaiser[b], M. Lucas[a]

[a] *Departamento Ingeniería Mecánica y Energía, Universidad Miguel Hernández, Avda. de la Universidad, s/n, 03202 Elche, Spain*

[b] *Departamento de Ingeniería Térmica y de Fluidos, Universidad Politécnica de Cartagena (Campus Muralla del Mar), Dr. Fleming, s/n, 30202 Cartagena, Spain*

[c] *Departamento Ingeniería de Sistemas y Automática, Universidad Miguel Hernández, Avda. de la Universidad, s/n, 03202 Elche, Spain*

Abstract

Cooling tower emissions are harmful for several reasons such as air polluting, wetting, icing and solid particle deposition, but mainly due to human health hazards (i.e. Legionella disease). blueThere are several methods for measuring drift drops. This paper is focussed on the sensitive paper technique, which is suitable in low drift scenarios and real conditions. The lack of an automatic classification method motivated the development of a digital image process algorithm for the Sensitive Paper method. This paper presents a detailed description of this method, in which, drop-like elements are identified by means of the Canny blueedge detector combined with some morphological operations. Afterwards, the application of a J48 decision tree is proposed as one of the most relevant contributions. This classification method allows to discern between stains whose origin is a drop and stains whose origin is not a drop. The method is applied to a real case and results are presented in terms of drift and PM_{10} emissions. This involves bluethe calculation of the main features of the droplet distribution at cooling tower exit surface in

*Corresponding author
Email address: j.ruiz@umh.es (J. Ruiz)

terms of drop size distribution data, cumulative mass distribution curve and characteristic drop diameters. The Log-normal and the Rosin–Rammler distribution functions have been fitted to the experimental data bluecollected in the tests and it can been concluded that the first one is the most suitable for experimental data among the functions tested whereas the second one blueis less suitable. Realistic PM_{10} calculations blueincludes the measurement of drift emissions and Total Dissolved Solids as well as the size and number of drops. Results are compared to the method proposed by the blueU.S. Environmental Protection Agency assessing its overestimation. Drift emissions have found to be the 0.0517% of the recirculating water, which is over the limit of Spanish standards (0.05%).

Keywords:
Cooling tower emissions, Sensitive Paper, Canny edge detector, Log-normal distribution function

---

Nomenclature

A_p	sensitive paper surface (m^2)
A_T	cooling tower exit surface (m^2)
C_C	Cunningham slip correction factor
$d_{0,1}$	10% spray proportion diameter, (m)
$d_{0,5}$	median diameter, (m)
$d_{0,9}$	90% spray proportion diameter, (m)
d_{32}	Sauter mean drop diameter, (m)
d_d	drop diameter, (m)
d_p	solid particle diameter, (m)

d_s	stain diameter, (m)
$\hat{d}$	Rosin–Rammler mean drop diameter, (m)
D	cooling tower drift
E_c	quadratic error
f	percent of solid mass emissions with $d_d \leq 10$ μm
L	characteristic dimension, (m)
$\dot{m}_d$	mass flow measured by the sensitive paper, (kg s^{-1} m^{-2})
$\dot{m}_s$	mass flow exiting the cooling tower, (kg s^{-1})
$\dot{m}_w$	mass flow sprayed by the cooling tower, (kg s^{-1})
M_{Logn}	Log-normal cumulative mass fraction
M_{RR}	Rosin–Rammler cumulative mass fraction
n	Rosin–Rammler shape factor
n_p	number of papers
N	number of drops
Stk	Stokes number
t	exposure time, (s)
v	relative velocity between the particle and the fluid stream, (m s^{-1})
Greek symbols	
ε	collection efficiency
λ	Log-normal mean value
μ	dynamic viscosity, (kg m^{-1} s^{-1})
ρ	density, (kg m^{-3})
σ	Log-normal standard deviation
ψ	difference between calculated and experimental values
Subscripts	

a	fluid
TDS	total dissolved solids
w	particle
Superscripts	
$-$	averaged value
Abbreviations	
EPA	Environmental Protection Agency
FN	False Negatives
FP	False Positives
PM_{10}	Particulate Matter of 10 microns in diameter or smaller
RS	Relative Span
SF	Spread Factor
SP	Sensitive Paper
TN	True Negatives
TP	True Positives
TDS	Total Dissolved Solids

1. Introduction

Cooling systems have become essential in the daily bluelife. In fact, air conditioning is directly responsible for the increase of the energy demand of the blueservice industry. The increment of the installed power for applications of cooling systems has lead to an increase of the blueconsumption peak. Depending on the application, different cooling technologies should be applied in order to evacuate heat of a refrigeration cycle. Among all the existent solutions, two bluetypes can be distinguished: those which employ atmospheric air as condensation element (air condensation systems) and those which use recirculation water to accomplish the same task (evaporative cooling systems). blue The main difference between water and air condensation systems is that the condensing temperature and pressure of the water cooled refrigerant systems is lower than the condensing temperature and pressure of the air cooled refrigerant systems. The fact that the condensing temperature and pressure of the water is lower means that, for the same cooling capacity, their energy consumption is also lower. Furthermore, an increase of CO_2 emissions to atmosphere is related to the lower energy efficiency of the air condensation systems.

The most bluewidely used water condensation systems is the cooling tower. The operation principle of cooling towers consists of an energy exchange between water and air flows. During the process, the waterflow descends from the top of the tower to the tower basin. Meanwhile, a fan produces a vertical counterflow of the air in the opposite direction of bluewater. Water transfers heat to air producing the evaporation of a small part of the water and the cooling of the rest. This heat extracted from water is evacuated from the tower by means of the air flow.

In practice, it is possible that an extremely small part of water escapes from the tower as drops. The total quantity of drops taken away is known as drift. This drift means a water loss but also may produce several negative consequences: wetting, icing, salt deposition, and related problems such as damage to equipment or to vegetation (Talbot, 1967), as well as human health hazards.

When studying cooling tower emissions, it must be taken into account that drift is not pure water bluesince it has the same composition of the recirculating water of the cooling tower. Therefore, drift will contain any impurities present in the recirculating water. This particulate matter will blueremain in the air and possibliy deposit to the ground when the water of drops evaporates. AP–42 (EPA, 1995) describes a method to blueestimate the emission of particulate matter. This technique makes two assumptions: the total disolved solids (TDS) are 11500 ppm and all disolved solids contained in drift are PM_{10}, that is to say, all diameters of solid particles are below 10 μm. However, in the work of Reisman and Frisbie (2002), they considered that PM_{10} is unrealistically modelled and thus blueproposed a more realistic method for estimating PM_{10} emissions from cooling towers. This ambiguity led to consider the experimental measurement of the particle matter emissions. This is tackled by measuring the TDS present in the recirculating water of the plant, the drift emitted and the size of the drops in the drift.

Among the problems related to cooling towers, Legionellosis is the most relevant. Legionellosis is caused by the Legionella, a bacterium whose habitat is the stagnant water. This bacterium proliferates specially in the presence of organic matter, temperatures between 20°C and 45°C, stagnant water or with low circulation and oxygen. The spread of this bacterium is probable bluedue to aerosols in the system. In the case of cooling towers having insalubrious conditions (due to inappropriate maintenance), Legionella can be present in the water of the tower basin. If some drops escape from the tower (drift), Legionella will be spread. In fact, there is a risk of inhalation depending on the size of the drops. In this way, it is necessary blueto develop a measurement technique that characterizes the bluequantity of drift as well the size of the drops. In Spain, the RD 865/2003 (BOE, 2003) establishes a maximum drift of 0.05% of the circulating water in the system. However, no method to measure this drift is mentioned.

In the literature, some methods to measure drift have been proposed (Lucas et al., 2012). Among these techniques, some countries have adopted one of them becoming a reference method. The method adopted by the British Standard BS 4485.2 (BS, 1988) and by the Japenese Industrial Standard JIS B 8609 (JIS, 1981) is the Thermal Balance Method. Other method is the one described in the Australian Standard AS 4180.1 (AS, 1994) named bluethe Chloride Balance Method. The American Cooling Technology Institute uses the Isokinetic Drift Test Code ATC 140 (CTI, 2011) and also refers to Sensitized Surface Methods. This methodology is described by Wilber and Vercauteren (1986).

blueRegarding the advantages of sensitive surface methods, the price is certainly the largest factor since sensitive papers are quite cheap compared to any device employed in drift measurements. Another strong point is the method capability of providing distributions of size and number of the drops collected. It presents, however, some disadvantages such as that it is impossible to discern between drift and the condensed water produced by the mixture of the hot saturated flow exiting the tower and the cold and dry flow outside. It does not allow to discern between specific chemical tracers neither. Meanwhile, laser techniques are also capable of providing accurate drop distributions (size and number of drops) but besides the price, they are not capable to perform field measures and are therefore most suitable for laboratory conditions.

Regarding the mentioned measuring methods, some comparative evaluation has been described in the literature. Roffman and Van Vleck (1974); Chen and Hanna (1978) presented a state of art bluereview of measuring techniques for drift and deposition and a comparison between them. The most detailed comparison of methods was carried out by Golay et al. (1986). They described numerous techniques and devices to measure cooling tower drift emissions, diverse in terms of sophistication, basic principles of operation and measurement capabilities. The results indicated that no single device is superior to the alternatives over the entire range of cases tested. Methods performing best under low water loading conditions utilize sensitive surface techniques. Methods performing best under high water loading conditions include the isokinetic mass sampling and chemical balance techniques. Additionally, Missimer et al. (1998) studied the relationship between Sensitive Paper and HGBIK drift measurements. The results showed similar results in both methods since the drift rate computed by the Sensitive Paper method was approximately 12% higher than the average rate estimated by the HGBIK method.

blueIn the current study, following the conclusions of Golay et al. (1986) the sensitive paper technique has been selected as the most suitable method to measure the drift bluefrom cooling towers with low levels of drift. This technique not only provides a quantitative drift value but also a qualitative information about droplet size distribution. Cizek and Novakova (2011) blueclassified the sensitive paper method as one of the most suitable for real world conditions.

The information can be extracted from sensitive papers by means of different techniques. First experiences to this method used a methodology to measure the number of drops captured by the sensitive papers. Particularly, in these techniques a human supervisor performed tasks of classification, evaluation and measurement. Later, some digital tools were employed. For example, Wilber and Vercauteren (1986) used the Digital Pen and therefore the extraction of information was speeded up. In the recent years, the bluemanual methodology has made way to an automatic process due to the development of hardware and image processing techniques. In this work digital processing is applied in order to identify droplets in sensitive papers.

Regarding the detection of droplets on an image, some previous work has been performed. Bras et al. (2009) tried to model and validate liquid-liquid systems. They used a camera to capture an image of droplets on a fluid. In this case, the Hough Transform is used to detect drop-like structures and then recall-precision curves evaluate the accuracy of the droplets detection. Digital imaging processing was also used by Terblanche et al. (2009) to measure drops inside a cooling tower. Images are converted into white blobs over black background and the number of pixels included in each drop is counted in order to obtain the equivalent spherical diameter. This work aimed to determine the drop size distribution beneath different fills. As conclusion, they stated that the Rosin–Rammler distribution curve is not a suitable solution to fit to experimental data. Particularizing to the sensitive paper technique, Cruvinel et al. (1996) applied imaging processing to detect drops on sensitive papers using the Hough Transform and then drops are identified by means of correlation with a patron. Hoffman and Hewitt (2005) extracted information from sensitive papers by means of three different methods and computed the correlation between them in terms of several definitions of the diameter that represents the drops distribution.

In this paper, digital processing to identify drops is tackled in three steps: detection, description and classification. Detection implies identification of drop-like elements. Then, these drops should be described and therefore two non-dimensional features are propoposed. Finally, it is necessary blueto have an automatic classication method which is able to identify which stains come from real drops. In this work, some classification methods are tested in order to find the most suitable one for this purpose and the automation of this classification process is also presented.

The main objective of this paper is to describe the experimental setup and the techniques to measure the emissions of a cooling tower: drift and PM_{10}. This study is applied to a real case and the results are discussed according to Spanish standards. The main features of the droplet distribution at cooling tower exit surface are presented in terms of drop size distribution data, cumulative mass distribution curve and characteristic drop diameters. Additionally, it is considered necessary to experimentally meassure the particle matter emissions. Finally, this work also aims to find a distribution function that fits suitably to the experimental data. The goodness of the fits is discussed through the quadratic error calculation.

2. Method

2.1. Introduction

Sensitive paper (SP) techniques are based on the collection of droplets taken away from a cooling tower by the air flow and collected by inertial impact thereof on a sensitive surface placed perpendicular to the flow. This paper is chemically treated (soaked in a solution of Potassium Ferricyanide $[K_3Fe(CN)_6]$, dried and dusted with Ferrous Ammonium Sulfate $[Fe(NH_4)_2(SO_4)_2 \cdot 6H_2O]$ powder). When a drop impacts on it, it creates a blue stain on the pale yellow background paper. The size and shape of the stain depends on the speed of impact and the original diameter of the drop. If the papers are exposed perpendicularly to the airflow, the stain will have a circular or nearly circular shape. The stain-drop size relationship can be known by calibrating the water-sensitive paper system by generating a known droplet's distribution with a generator of monodisperse drops in different size ranges and rating them. The manufacturer provides a calibration curve where the spread factor (relation between the original diameter of the drop and the stain produced on the paper) is supplied. The sensitive paper with stains generated by drops of water, undergoes a process of scanning the image. First, the paper must be digitized in order to pass this information to the computer, which through an image processing program and analysis will be able to count, measure and classify the stains according to their size. This analysis leads to a droplet distribution by size based upon the calculation of the droplets diameters through the area covered by each stain. The procedure to experimentally determine the drift emitted by a cooling tower based on sensitive paper techniques involves to cover three main steps: carrying out the tests, image processing and drift calculation. Each step is also divided in tasks; in the first step, number of papers and exposure time, carrying out the tests and storing the papers are carried out, in the second step, the scanning of the papers and the image processing using a computer are performed and finally, in the third step the cooling tower drift is calculated.

2.2. Carrying out the tests

Prior to performing the drift tests, the number and position of the papers and exposure time shall be defined. The number of papers placed on cooling tower's exit surface will be selected with the purpose of gathering the maximum number of samples (papers) without influencing the measure. In rectangular cross-sectioned cooling towers rectangular papers and grid structure is recommended whereas in circular cross-sectioned cooling towers, circular papers forming concentric circles are the most proposed distribution. Moreover, the exposure time of the papers in the tests is the most important factor to be taken into account in the first step. Thus, a trial test to decide the best time has to be performed. The time will be considered as optimal when obtaining the maximum number of stains without the overlapping between drops nor the edges paper becoming green due to the flow of moist air concentrated in that area. To establish the exposure time a compromise solution will be adopted in spite of the two conditions mentioned previously. Once the number of papers and exposure time have been set, tests are carried out and the papers are stored. The procedure to perform the tests and store the papers is detailed in section 3, where the SP method is applied to a real case.

2.3. Image processing

The digital processing of the papers is the second step of the method and covers from the scanning to the processing of the papers.

First, sensitive papers are digitized by means of a high resolution scanner. Then, all the stains present in the paper (coming or not from a real droplet) are detected, trying to extract as much information as possible from them. Next step is to describe these stains, and therefore some features should be selected so that drop-like stains are properly characterized. Finally, a classifier is employed to discern between "drop","no drop" and "multiple-drop", based on the selected features. In the following, the process is described in detail.

Stains detection. This section explains how the digitized paper is processed in order to extract the maximum amount of information. The sensitive paper images are digitized in BMP format and have RGB information in their original form. However, for computing reasons, the work is performed with gray-scale images. As a consequence the image is separated into the R-, G- and B-channels and the R-channel is chosen as the most adequate. As it can be observed in figure 1, the R-channel presents more information than the B-channel and is more contrasted than the G-channel. As a result, the R-channel presents good defined stains in a well contrasted background and keeps all the necessary information.

Then, by means of the OpenCV library is used to extract all possible droplets from the paper. Particularly, drop-like stains are identified by means of the Canny edge detector, (Canny, 1986). This detection process in enhanced by two morphological operations: dilate and erosion, furthermore the contours are filled. All this operations eliminate noise and close the detected contours so that well-defined droplets are obtained. Figure 2 shows the droplets detected after Canny and the morphological operations.

Next step is to define feaures that describe the drop-like appearance of these stains and to train a classifier based on these features.

Description. Once the stains are detected, the next step is to describe them. For that reason, previous to classification, the selection of the features that characterize a drop are selected. These features are desirable to be non-dimensional so that this study can be extended to other cooling tower typologies or other structural elements. Under these requirements, "Roundness" and "Hu Moments" were selected as classifying features. "Roundness" is proportional to the perimeter and area coefficient, whereas "Hu Moments" are dimensionless inertia moments based on the inertia moment of the detected drop.

Then, a training step is required in order to obtain the classifier based on the features and a training set. The training step as well as the classification step have been carried out by means of the WEKA software, (Hall et al., 2009). After a manual supervision, a training data set of 1037 samples was extracted from the papers. Moreover, different combinations of the classifying features testing "Roundness" and "Hu Moments" form 1 to 7 order have been considered. As a result of these tests, only "Roundness" and "1st Hu Moment" are significant features in the classification of the stains.

Classification. The stage of classification aims to obtain a reliable method which is able to identify different classes in the data obtained. Particularly, three different classes have been defined for classification of stains as shown in figure 3. Stains coming from real drops belong to the “drop” class; those with a different origin are associated to the “no drop” class and, additionally, the case in which multiple drops overlap is also taken into account. This anomaly is tackled approximating those drops to a unique one, which is identify as the “multiple-drop” class.

The goodness of a classification method can be analyzed according to two criteria: a success rate measure and a confusion matrix. The success rate measures the percentage of correct classification cases, whereas the confusion matrix shows all the associations made. The general form of this confusion matrix is shown in table 1. The diagonal represents the true positives (TP), i.e., positive cases correctly classified and true negatives (TN), i.e., negative cases correctly classified. We consider that positive cases are “drop” and “multiple-drop” and the negative case is “no drop” class. Then, out of the diagonal there are the false positives (FP), i.e, negative cases classified as positive and false negatives (FN), i.e., positive cases classified as negative. In the ideal situation, would obtain a diagonal matrix. However, in practice values out of the diagonal are obtained. In this situation, it is desirable to obtain FP rather than FN, which means that some samples are incorrectly classified as drops. That is to say, the preference is not to lose information coming from real drops. In this work, two classification methods have been tested: Bayesian classifier and decision tree (J48). Table 2 shows the results obtained for each classification method. The results are presented in terms of success rate and confusion matrix, whose general form is explained in table 1. It can observed that J48 method obtains a higher success rate. Moreover, comparing the confusion matrix in both methods, J48 obtained

		Classified as		
		Drop	Multiple-drop	No drop
Actual class	Drop	TP	FP	FN
	Multiple-drop	FP	TP	FN
	No drop	FP	FP	TN

Table 1: Schematic description of the confusion matrix.

Type of classifier	Bayesian	Decision tree (J48)
Success rate (%)	92.7676	94.0212
Confusion matrix	$\left[\begin{array}{cccc} & a & b & c \\ a & 775 & 8 & 0 \\ b & 12 & 187 & 0 \\ c & 17 & 38 & 0 \end{array}\right]$	$\left[\begin{array}{cccc} & a & b & c \\ a & 772 & 11 & 0 \\ b & 7 & 192 & 0 \\ c & 7 & 37 & 11 \end{array}\right]$

Table 2: Success rate and confusion matrix for Bayesian and decision tree (J48) classifier. Subscript "a" stands for drop, "b" multiple-drop while "c" denotes no drop.

the highest success rate. In addition, J48 has a higher rate in false positives (FP) than in false negatives (FN), as it was preferable. This means that J48 classifies wrongly stains as drops better than losing real drops. Given these results, it is considered that J48 is a suitable classifier using "Roundness" and "1st Hu Moment" as classifying features. We also consider that the non gaussianity of the classifying features justifies that the results obtained by the Bayesian method are less satisfactory. As a result of the drop detection and classification steps, a vector which includes the diameters of the stains that have been originated by drops is obtained (classified as "drop" or "multiple-drop") detected in each sensitive paper.

2.4. Data processing

The image processing technique provides only the surface covered by the stains, but not the diameter of the drops which caused them. Thus the drop-stain relationship is employed. The calibration curve is supplied by the manufacturer where the spread factor (SF), defined in equation (1) is given.

$$\mathrm{SF} = \frac{d_s}{d_d} \tag{1}$$

Tests have been performed using the Teejet model of hydrosensitive paper with dimensions of 52 x 76 mm, manufactured by Syngenta Crop. Protection AG., and distributed by Spraying Systems Co. The calibration curve is shown in figure 4. The spread factor alongside the stains vector provided in the previous step allow the calculation of the drop's diameter which has caused the stain.

Next, the collection efficiency is used to correct the error in such measurements where only the particles that impact on the collection surface are taken into account, not considering those particles which, because of their size or velocity, have been carried by the airflow.

A particle suspended in a fluid stream tends to move in a straight line because of its inertia. However, when the fluid meets an obstacle, the particle tends to move towards the obstacle and depending on factors such as particle velocity or particle diameter, it will end up hitting the obstacle or being deflected by the change of flow direction. Therefore, a parameter known as collection efficiency of the obstacle is defined. The inertial impactors, such as water-sensitive papers, have been studied extensively through theoretical and experimental studies (Ranz and Wong, 1952; Golovin and Putnam, 1962; May and Clifford, 1967).

The collection efficiency ε, is defined as the ratio between the number of particles captured, compared to the total of particles injected into the projected surface of the collector object, as shown in equation (2).

$$\varepsilon = \frac{N_{trapped}}{N_{inyected}} \tag{2}$$

The Stokes number is the non dimensional parameter which appears after performing a dimensional analysis to the problem of the collection efficiency by inertial impact.

$$\mathrm{Stk} = \frac{\rho_w\, d_d^2\, v\, C_C}{18\, \mu_a\, L} \tag{3}$$

The characteristic dimension, L, is usually determined as the projection of the width of the object in the direction perpendicular to the flow. The Cunningham correction factor should be applied to take into account that the Stokes law ceases to be accurate when the particle size is similar to the mean displacement of free gas molecules containing the particles. This correction factor is close to unity, and hence negligible for particles in air at normal temperature and pressure up to 1 μm in diameter (Baron and Willeke, 2001). With smaller particles or low pressure conditions, the Cunningham correction factor can be important. Figure 5 shows the collection efficiency curve for ribbons, from the experimental data of May and Clifford (1967).

Having taken into account the spread factor and the collection efficiency, drift can be calculated for each water-sensitive paper by equation (4).

$$\dot{m}_{d,i} = \frac{\rho_w\, \pi}{6\, A_p\, t} \sum_{i=1}^{N} d_{d,i}^3\, \varepsilon^{-1} \tag{4}$$

Where ε^{-1} is the associated collection efficiency for each $d_{d,i}$.

The mass flow of water that escapes through the outlet section of the tower, is calculated as:

$$\dot{m}_s = \frac{A_T}{n_p}\sum_{i=1}^{n_p}\dot{m}_{d,i} \tag{5}$$

Finally, drift is calculated as the ratio between the mass flow of water escaping from the tower $\dot{m}_s$ and the total mass flow sprayed $\dot{m}_w$:

$$D = \frac{\dot{m}_s}{\dot{m}_w} \tag{6}$$

3. Experimental apparatus

In order to test the method, the amount of drift emitted by a bluecommercial cooling tower was experimentally calculated. The facility where the experiments were carried out, shown in figure 6, is assembled on the roof of a laboratory at the Universidad Miguel Hernández in the city of Elche, southeast of Spain. The main device of this test plant is a forced draft cooling tower with a cross-sectional area of 0.70 x 0.48 m^2, a total height of 2.597 m and a packing section that is 1.13 m high. The packing material consists of fiberglass vertical corrugated plates. Water pressure nozzles are used to distribute the water uniformly over the packing and the air is circulated counter-flow by an axial fan. The drift eliminator presents a zig-zag structure and consists of stainless steel plates separated at distance of 47 mm. The fan's motor is equipped with a variable speed control, which allows the change of the air mass flow rate. Sprayed water mass flow rate can be changed manually by means of a balancing valve. Drift was calculated for nominal conditions (5200 l/h of mass flow rate and 50 Hz for the frequency switcher). A general-purpose data-acquisition system was set up to carry out

Magnitude	Day 1 (07/27/2011)	Day 2 (09/20/2011)
Water mass flow (kg/s)	1.424	1.431
Ambient temperature (°C)	26.20	23.10
Output temperature (°C)	23.56	20.16
Ambient relative humidity (°C)	46.25	50.01
Output relative humidity (%)	99.23	97.38
Inlet water temperature (°C)	20.94	18.88

Table 3: Averaged ambient and operating conditions registered during the tests.

the experimental tests. All data was monitored with an HP 34970A Data Acquisition Unit. Specific software was written and compiled for the system, supporting up to 36 inputs, with 16 bits A/D, 9600 bands transmission speed and programmable gain for individual channels.

Five sets of experiments were carried out in order to ensure the repeatability of the results. The first and second tests were performed during the morning of July the 27$^{\text{th}}$, while the third, fourth and fifth took place on September the 20$^{\text{th}}$ (2011). The main parameters of the ambient and operating conditions are shown in table 3.

To carry out the tests, the procedure defined in section 2.2 for the drift calculation is followed here. Once the cooling tower is operating under stationary conditions (it requires at least half an hour in order to the drift eliminator to become saturated), the number of the papers was set to nine, placed at regions separated into three zones accordingly to the north-south axis of the tower. With the purpose of standardize the measures, an attachment for the cooling tower was built. This device, made of PVC, allows the paper supports be fitted always in the same position and the tests not to be influenced by the wind. The setup described above (number and position of papers) has been taken as a reference for all the tests carried out. Regarding the interval, trial tests showed three seconds to be the optimal exposure time according to the compromise solutions criterion.

Having selected the exposure time, the real tests were performed following the sequence southern zone, central zone and northern one. Tests were performed using a rod where a PVC plate was used as a support for the papers. At the beginning of the test, the rod's shaft was to be held keeping the sensitive papers surface back to the flow at all times. In the start of the test the shaft of the rod has to be rotated 180° to place the paper surface perpendicular to the flow of moist air. After the selected time has passed, the rod is turned back so that the flow of moist air does not blow on the paper's yellow face, and it is immediately removed from the exit surface for droplets not to slide on it and not falling more drops on it. Figure 7 shows the cooling tower exit surface where the PVC support has been attached with the PVC plates used. Finally the papers were stored when they were completely dry. They were removed from the support taking great care not to damage nor contaminate them. And then, for the environmental conditions not to affect the papers, they were stored in vacuum bags. This solution is very practical, and also gives very good results because the papers remain unchanged the time it takes to begin the scanning process.

Regarding the scanning process, the equipment used is a professional photo scanner CanonScan 9950F model. It is a plain scanner with 4800 x 9600 dots per inch of optical resolution. As for the scanning parameters, it

Test run	1	2	3	4	5
$\sum \dot{m}_{d,i}$ (kg s^{-1} m^{-2})	0.017149	0.015745	0.020384	0.019225	0.017014
$\dot{m}_s$ (10^{-4}) (kg s^{-1} m^{-2})	7.0825	6.50263	8.41829	7.93957	7.02667
D (%)	0.049722	0.045651	0.058828	0.055483	0.049103

Table 4: Drift calculation results for the test runs 1 to 5.

was decided to scan the papers with the highest possible resolution of the scanner (4800 pixels per inch (5.291 μm / pixel)) to lose as little information as possible. 24-bit true color has been selected for depth pixel, to get all the tonal changes in the paper. For processing these images with the computer, the BMP format was chosen. The scanning of the papers has been performed using the software provided by the scanner manufacturer. Finally the image process and drift calculation steps are performed.

4. Results and discussion

blueThe results obtained from the bluefive sets of experiments carried out in the experimental facility are bluedescribed in this section. These are presented in terms of drift emissions and characteristic diameters, proposed functions to fit experimental drop size distributions and PM_{10} emissions.

4.1. Drift emissions and characteristic diameters

Table 4 shows drift emissions calculated according to equations (4), (5) and (6), while figure 8 depicts the drop distribution data for the set of experiments.

Paying attention to drift results, they show that the averaged value of the drift taken away from the tower is D=0.0517% with and standard deviation of 0.00529%. This value is rather high compared to typical present-day manufacturers' guaranteed drift rates, which are on the order of 0.002% (EPA, 1995). As the Spanish standards allow cooling towers to emit a maximum of the 0.05% of the circulating water, it can be said that the cooling tower operating under nominal conditions with the eliminator fitted is over the limit allowed. In that case, to ensure that the standards are upheld, it would be strongly recommended to replace the eliminator with another with higher efficiency or to change the geometry (number and shape of laths) to achieve better efficiencies.

For many purposes and in order to characterize the ensemble of drops exiting the tower, which contain drops of different sizes, a single number is required. Sometimes, the median diameter, $d_{0,5}$, (50% of the drops are larger and 50% are smaller than the median, in mass or volume terms) is employed. Moreover, according to Hoffman and Hewitt (2005), two additional droplet size parameters that are commonly used to describe more of the distribution than the median alone are the $d_{0,1}$ and $d_{0,9}$. They describe the proportion of the spray volume (10% and 90%, respectively) contained in droplets of the specified size or less. Finally, the Relative Span (RS) is a measure of the width of the droplet spectra around the $d_{0,5}$ defined in equation (7).

$$\mathrm{RS} = \frac{d_{0,9} - d_{0,1}}{d_{0,5}} \tag{7}$$

In some cases, these diameters will suffice to describe the distribution, but because the drop surface area and volume are proportional to the square and cube of the diameter, respectively, a more complex description is required.

Test run	1	2	3	4	5
$d_{0,1}$ (mm)	0.0204	0.0218	0.0215	0.0206	0.0234
$d_{0,5}$ (mm)	0.0323	0.0326	0.0345	0.0344	0.0364
$d_{0,9}$ (mm)	0.0762	0.0779	0.0764	0.0746	0.0825
RS	1.7258	1.7202	1.5948	1.5710	1.6232
d_{32} (mm)	0.0319	0.0325	0.0333	0.0327	0.0357

Table 5: Calculated values for $d_{0,1}$, $d_{0,5}$, $d_{0,9}$, RS and d_{32} for the test runs 1 to 5.

A general mean diameter can be defined by

$$d_{pq} = \left[\frac{\sum_{i=1}^{N} d_{d,i}^{p}\, \varepsilon_i^{-1}}{\sum_{i=1}^{N} d_{d,i}^{q}\, \varepsilon_i^{-1}} \right]^{\left(\frac{1}{p-q}\right)} \tag{8}$$

According to Terblanche et al. (2009), the Sauter mean diameter represents mean diameter with the same ratio of volume to surface area as the entire ensemble. It corresponds to values of $p = 3$ and $q = 2$ in equation (8). The Sauter mean diameter (d_{32}) is probably the most commonly used mean as it characterizes a number of important processes. Chin and Lefebvre (1985) suggested that it is the best measure of the fineness of sprays.

Results of $d_{0,1}$, $d_{0,5}$, $d_{0,9}$, RS and the d_{32} are presented in table 5. As it can be observed, the sequence of diameters attending to its size is, as expected, $d_{0,9}$, $d_{0,5}$, d_{32} and $d_{0,1}$ (Williams, 1990). Since the standard deviation to mean value ratio of all of the parameters is lower than 5%, repeatability can be ensured.

4.2. Drop size distributions fits

blueIt is important to have experimental data that can be fitted to a theoretical model in order to best define a numerical model for predicting the dispersion and deposition of cooling tower drift. In the literature, some numerical models are available that have been evaluated using experimental data from several sources. Meroney (2006) and Lucas et al. (2010) used the experimental data taken from the bluestudy of Policastro et al. (1981) to validate their numerical dispersion and deposition results. They both employed the Rosin–Rammler function to fit the experimental data of the drops blueemitted from the cooling tower. However, according to Terblanche et al. (2009), fitting the Rosin–Rammler functions to experimental data does not provide consistent curve fits and blueshould be avoided. Nonetheless, they propose no bluealternative function.

In order to assess the conclusions reached by Terblanche et al. (2009) regarding the Rosin–Rammler function, and aiming to determine the most suitable function for fitting droplet distributions, the Rosin–Rammler, the Modified Rosin–Rammler and the Log-normal distribution functions have been fitted to the experimental data and the goodness of the fits has been bluedetermined through the quadratic error calculation.

A cumulative mass distribution is a distribution curve which gives measured cumulative mass fraction data as a function of drop diameters. blueThe cumulative mass fraction at a certain drop diameter is defined as the drop mass fraction of which the drop diameters are bluesmaller than that specific diameter. The Rosin–Rammler function is an empirical relation used to correlate measured cumulative mass distribution data, expressed as

$$blueM_{RR} = 1 - e^{-\left(\frac{d}{\hat{d}}\right)^n} \tag{9}$$

where the Rosin–Rammler mean drop diameter, $\hat{d}$, is obtained from the measured cumulative mass distribution at the diameter where the cumulative mass distribution is blue$1-e^{-1}$ while the shape factor, n, can be determined by an average of equation (10) for each drop diameter interval.

$$bluen = \frac{\ln(\ln M_{RR})}{\ln \frac{d}{\hat{d}}} \tag{10}$$

blueAs mentioned above, the Rosin-Rammler distribution has been found by others to not produce the best agreement with experiment data and other distributions are preferable. Here, the Modified Rosin–Rammler function is proposed, where the set of parameters $\hat{d}$ and n, have been selected in order to minimize the error between calculated and experimental results. Finally the Log-normal function, which according to Linmpert et al. (2001) is suitable for size distributions of aerosols, can be expressed as

$$M_{Logn} = \frac{1}{2}\left[1 + \operatorname{erf}\left(\frac{\ln d - \lambda}{\sqrt{2\sigma^2}}\right)\right] \tag{11}$$

where λ and σ are the mean and standard deviation, respectively, of the variable's natural logarithm and erf is the error function defined as

$$\operatorname{erf}(x) = \frac{2}{\sqrt{\pi}} \int_0^x e^{-t^2} dt \tag{12}$$

Figure 9 depicts the drop size distribution data and the cumulative mass bluedistribution curves for the tests carried out.

The goodness of the fits can be blueshown using the quadratic error calculation, E_c. blueThe magnitude, defined in equation (13), measures the ratio of the square difference between calculated and experimental values (ψ) to the number of drops (N).

$$E_c = \frac{\sum_{i=1}^{N} \psi_i^2}{N} \tag{13}$$

Test run		1	2	3	4	5
Rosin–Rammler	$\hat{d}$ (mm)	0.0381	0.0382	0.0402	0.0401	0.0427
	n	2.1833	2.2064	2.2570	2.2032	2.2816
	E_c	0.0040	0.0039	0.0034	0.0035	0.0039
Modified Rosin–Rammler	$\hat{d}$ (mm)	0.0513	0.0518	0.0520	0.0513	0.0556
	n	1.2694	1.3273	1.3660	1.3470	1.3779
	E_c	0.0035	0.0038	0.0029	0.0025	0.0035
Log-normal	λ	-3.3015	-3.2806	-3.2689	-3.2840	-3.2009
	σ	0.5971	0.5776	0.5662	0.5720	0.5647
	E_c	0.0011	0.0013	0.0010	0.0009	0.0010

Table 6: Fitting parameters $\hat{d}$ and n for Rosin–Rammler and Modified Rosin–Rammler functions and λ and σ for Log-normal function; Quadratic error results.

The fitting parameters $\hat{d}$ and n for both Rosin–Rammler functions, λ and σ for the Log-normal and the values of the E_c for the three distributions, are presented in table 6.

Results show that the maximum error blueoccurs for the Rosin–Rammler function followed by the modified Rosin–Rammler and the Log-normal function. This fact corroborates the conclusions reached by Terblanche et al. (2009), bluewho advised to avoid the Rosin–Rammler function. In the present case this functions bluehas the maximum error between calculated and experimental data for all of the tests performed. Despite bluethe fact that the function is able to predict correctly the beginning and the centre of the curve, it ceases to be accurate for the blueasymptotic behaviour at the end of the curve. blueThe Modified Rosin-Rammler distribution was proposed in order to correct the problem. In this function, the mean and shape factors ($\hat{d}$ and n) are calculated blueby minimizing the error criterion. However, despite bluethe fact that this function bluebetter fits the experimental data than the Rosin–Rammler function, specially at the asymptote, it fails at the centre of the curve. Meanwhile, the Log-normal bluehas the minimum quadratic error for all the tests performed and predicts very well blueat all parts of the curve.

4.3. PM_{10} *emissions*

blueThe calculations of PM_{10} emissions are discussed in this subsection. The EPA (1995) AP-42 report states that the particulate matter constituent of the drift droplets may be classified as an emission because the direct contact between the cooling water and the air passing through the tower. blueA conservative method is proposed to calculate the PM_{10} emission factor, which can be estimated, (a), by multiplying the total liquid drift factor by the total dissolved solids (TDS) fraction in the circulating water and (b), by assuming that, once the water evaporates, all remaining solid particles are within the PM_{10} size range. blueThe values provided by AP-42 (EPA, 1995) for drift emissions and TDS in wet mechanical cooling towers are 0.02% and 11500 ppm respectively. However, Reisman and Frisbie (2002) proposed bluean alternate realistic method to calculate the PM_{10} emissions based upon the fact that not all the solids which escape through the tower are particles. They concluded that the AP-42 method (EPA, 1995) does not account for the droplet size distribution of the drift exiting the tower and hence this is a critical factor, as more than 85% of the mass of particulate in the drift from most cooling towers will result in solid particles larger than blue10 μm once the water has evaporated. Particles larger than blue10 μm are no longer a regulated air pollutant, because their impact on human health has been shown to be insignificant.

The procedure to calculate PM_{10} emissions according to Reisman and Frisbie (2002) is shown bluebelow.

$$\mathrm{PM}_{10} = \mathrm{PM}\, f = \dot{m}_s\, \mathrm{TDS}\, f \tag{14}$$

$$d_p = d_d \left(\mathrm{TDS} \frac{\rho_w}{\rho_{\mathrm{TDS}}} \right)^{\frac{1}{3}} \tag{15}$$

blueFor the present study, PM_{10} emissions have been calculated using the EPA (1995) AP-42 method, for the water mass flow rates shown in table 3 and the above given values of 11500 ppm for the TDS and 0.02% for drift emissions. blueAlso emissions have been calculated blueusing the Reisman and Frisbie (2002) method for the drift emissions presented in table 4 and a water density to TDS density ratio equal to 0.461. The TDS content has been estimated by blueusing the TDS observations for the make-up water (462 ppm) and multiplying them by blue3 cooling tower cycles of concentration (it usually ranges from 3 to 7 in the majority of cooling towers), for a total of TDS=1386 ppm in mass. The results of the bluecompararison of methods are shown in table 7.

As expected, results blueshow that the AP-42 method overestimates the PM_{10} emitted by the tower. The difference is about one order of magnitude. Results for the Reisman and Frisbie (2002) method show slightly differences between PM and PM_{10} emissions because bluethe quantity of TDS present in the water is low. Hence, once blueevaporated from the water, most of solid particles have diameters smaller than 10 μm. Thus the percent of solid mass

Test run	1	2	3	4	5
PM_{10} (10^{-6}) (kg $s^{-1})^a$	3.275	3.275	3.291	3.291	3.291
PM (10^{-6})(kg s^{-1})	0.982	0.901	1.167	1.100	0.974
f (%)	94.65	94.51	95.05	95.36	94.63
PM_{10} (10^{-6}) (kg $s^{-1})^b$	0.929	0.852	1.109	1.049	0.922

Table 7: PM, f and PM_{10} blueemissions calculations for the tests performed in the facility described in section 3. a) Calculated according to EPA (1995) AP-42 method; b) Calculated according to the Reisman and Frisbie (2002) method.

emissions bluewhose diameter is equal to, or smaller than 10 μm, f, is close to 100 %. blueHowever a difference would be found if the amount of TDS increases.

blueEven if the TDS content of the water increases, a scenario where PM_{10} emissions calculated according to EPA (1995) AP-42 method would be lower than PM_{10} emissions calculated according to the Reisman and Frisbie (2002) method seems unlikely. The reason is that, despite the fact that the PM to TDS ratio increases in a straight line, the PM_{10} to TDS ratio will begin to decline at some point because of the decreasing of f. At higher TDS, the drift drops will contain more solids, and so, even after evaporation, they will result in larger solid particles for any given initial droplet size. However, the difference between the EPA (1995) AP-42 and the Reisman and Frisbie (2002) PM_{10} emissions could have increased if a high-efficiency eliminator would have been used in our test experiments presented.

In conclusion it can be said that in the case presented in this paper the overestimation PM_{10} blueemissions by the method described in blueAP-42 (EPA, 1995) was found. blueIt is therefore recommended that a real calculation be performed of the PM_{10} emissions because factors such as the drift rate or the TDS value are subject to change depending on the facility where the drift is measured. Thus, the necessity of measuring not only TDS and drift but the distribution of diameters (size and number) is highlighted. In this sense the sensitive paper has proven to be suitable for the purpose.

5. Conclusions

This paper aims to describe the experimental setup and the techniques to measure the emissions of a cooling tower using the sensitive paper method. blueThe digital image process developed in order to measure the emissions is described. For that purpose sensitive papers blueare scanned after performing a drift test to obtain a digital image. Drop-like elements are identified by means of the Canny edge detector enhanced by some morphological operations (dilate, erosion and filling). To identify those stains bluewhose origin is a bluedrop, a classification method based upon two non-dimensional characteristics of the droplets (roundness and the 1^{st} Hu Moment) is proposed. This classification method, bluethe J48 tree, was selected after it was found to achieve the highest success rate. It is also capable of dealing with anomalies such as overlapping drops, classifying them as a multiple drops. blueThis classification method has proven to be one of the most relevant contributions of this work.

The application of the method to a real case has blueyielded estimates of emissions of droplets and distribution data curves blueand PM_{10} blueemissions, and can be summarized as follows. Drift emissions of the tower operating under nominal conditions are D=0.0517%. blueThis drift emission measurement is over the Spanish standard limits (0.05%). Therefore replacing the drift eliminator for another with higher efficiency would be advisable, blueespecially because today technologies can guarantee lower drift rates. The drop size distribution calculated in terms of characteristic diameters ensures the repeatability of the results even measured in different ambient conditions. The influence of operating conditions shall be studied in future works.

blueCorrelations for the cumulative mass distribution have been derived from the observations and three functions have been fitted to them. The goodness of the fits has been blueestimated through the quadratic error calculation. blueThe Log-normal distribution function has proven to yield the best fits, ($\bar{E}_c$=0.00106) better than bluethe Modified Rosin–Rammler function ($\bar{E}_c$=0.00324) blueand the Rosin–Rammler ($\bar{E}_c$=0.00374).

bluePM_{10} emissions have also been calculated according to the AP-42 (EPA, 1995) and Reisman and Frisbie (2002) methods. blueThe overestimation of the PM_{10} emissions calculation by the EPA method is assessed. It is strongly recommended that a separate calculation be performed for each cooling tower because factors such as drift rate and f can be modified depending on the drift eliminator blueinstalled in the tower or the amount of TDS present in the water. As this calculation requires quantitative (amount of drift) and qualitative (size and number of drops) information, sensitive surface methods are suggested to measure PM_{10} in real facilities. blueThese statements are mainly based on analysis of observations from the research apparatus presented in the section 3 and, despite the fact that the cooling tower is operating in the typical operating cooling tower conditions, there is a future need to test the sampling methods and the drop size distribution formulas with independent data. blue

6. Acknowledgements

The authors acknowledge the financial support received from the Spanish Government, through the Projects ENE2010-21679-C02-01 and 02 and by FEDER (Fondo Europeo de Desarrollo Regional).

References

AS, 1994. AS-4180.1. Drift loss from cooling towers; Laboratory measurement. Part 1: Chloride balance method. Standards Australia.

Baron, P., Willeke, K., 2001. Aerosol measurement: Principles, Techniques and Applications. 2nd Edition. Editorial John Wiley and Sons Inc.

BOE, 2003. RD 865/2003. Hygienic-sanitary criteria for the prevention and control of legionellosis. Ministry of health and consume.

Bras, L., Gomes, E., Ribeiro, M., Guimaraes, M., 2009. Drop distribution determination in a liquid liquid dispersion by image processing. International Journal of Chemical Engineering, 6–6.

BS, 1988. BS–4485.2. Water cooling towers. Part 2: Methods for performance testing. British Standards Institution.

Canny, J., 1986. A computational approach to edge detection. IEEE Transactions on Pattern Analysis and Machine Intelligence PAMI-8, 679–698.

Chen, N., Hanna, S., 1978. Drift modeling and monitoring comparisons. Atmospheric Environment (1967) 12, 1725–1734.

Chin, J., Lefebvre, A., 1985. Some comments on the characterization of drop-size distribution in sprays. In: Proceedings of ICLASS-85. Brazil.

Cizek, J., Novakova, L., 2011. New methods for drift eliminators performance evaluation. CTI journal 32, 32–40.

Cruvinel, P., Minatel, E., Mucheroni, M., Vieira, S., Crestana, S., 1996. An automatic method based on image processing for measurements of drop size distribution from agricultural sprinklers. In: IX SIBIGRAPI. Brazil.

CTI, 2011. ATC-140. Isokinetic Drift Measurement Test Code for Water Cooling Tower. Cooling Technology Institute.

EPA, 1995. AP–42. Compilation of air pollutant emission factors. United States. Environmental Protection Agency. Office of Air Quality Planning and Standards.

Golay, M., Glantschnig, W., Best, F., 1986. Comparison of methods for measurement of cooling tower drift. Atmospheric Environment 20, 269–291.

Golovin, M., Putnam, A., 1962. Inertial impaction on single elements. Ind. Eng. Chem. Fund 1, 264–273.

Hall, M., Frank, E., Holmes, G., Pfahringer, B., Reutemann, P., Witten, I. H., 2009. The weka data mining software: an update. SIGKDD Explor. Newsletters 11 (1), 10–18.

Hoffman, W., Hewitt, A., 2005. Comparison of three imaging systems for water-sensitive papers. Applied Engineering in Agriculture 21 (6), 961–964.

JIS, 1981. JIS B 8609. Performance tests of mechanical draft cooling tower. Japanese Industrial Standard.

Linmpert, E., Stahel, W., Abbt, M., 2001. Log-normal distributions across the science: Keys and clues. BioScience 51 (5), 341–352.

Lucas, M., Martínez, P., Ruiz, J., Kaiser, A., Viedma, A., 2010. On the influence of psychrometric ambient conditions on cooling tower drift deposition. International Journal of Heat and Mass Transfer 53 (4), 594–604.

Lucas, M., Martínez, P., Viedma, A., 2012. Experimental determination of drift loss from a cooling tower with different drift eliminators using the chemical balance method. International Journal of Refrigeration 35 (6), 1779 – 1788.

May, K., Clifford, R., 1967. The impaction of aerosol particles on cylinders, spheres, ribbons and discs. In: Ann. Occup. Hyg. Vol. 10. Great Britain, pp. 83–95.

Meroney, R., 2006. CFD prediction of cooling tower drift. Journal of Wind Engineering and Industrial Aerodynamics 94, 463–490.

Missimer, J., David, P., Wheeler, E., Hennon, K., 1998. Between SP and HG-BIK Drift Measurement Results - New Data Creates a Need for a Second Look. Cooling Technology Institute., Ch. Technical Paper. T-98-16.

Policastro, A., Dunn, W., Berg, M., Ziebarth, J., December 1981. The chalk point dye tracer study: validation of models and analysis of field data. Vol. 4-6. Proceedings of Second Conference on Waste Heat Management and Utilization, pp. 686–719.

Ranz, W., Wong, J., 1952. Impaction of dust and smoke particles on surface and body collectors. Ind. Eng. Chem. 44 (6), 1371–1381.

Reisman, J., Frisbie, G., 2002. Calculating realistic PM_{10} emissions from cooling towers. Environmental Progress 121 (2), 127–130.

Roffman, A., Van Vleck, L., 1974. The state-of-the-art of measuring and predicting cooling tower drift and its deposition. Journal of the Air Pollution Control Association 24 (9), 855–859.

Talbot, J., 1967. A review of potential biological impacts of cooling tower salt drift. Atmospheric Environment 13, 395–405.

Terblanche, R., Reuter, H., Kröger, D., 2009. Drop size distribution below different wet-cooling tower fills. Applied Thermal Engineering 29, 1552–1560.

Wilber, K., Vercauteren, K., 1986. Comprehensive drift measurements on a circular mechanical draft-cooling tower. Cooling Technology Institute., Ch. Technical Paper. T-86-01.

Williams, A., 1990. Combustion of Liquid Fuel Sprays. Butterworths, London.

7. Captions for figures

Figure 1: (a) Original image, (b) R-channel, (c) G- channel and (d) B-channel.

Figure 2: (a) Original image and (b) processed image.

Figure 3: Data types for the stains detected. a) “No Drop”, b) “Drop” and c) “Multiple Drop”.

Figure 4: Spread factor curve for Teejet 52 x 76 mm paper.

Figure 5: Experimental impaction efficiency of ribbons provided by May and Clifford (1967) and schematic arrangement of particle deposition on sensitive papers.

Figure 6: Arragement of the pilot test facility assembled at Universidad Miguel Hernández, Elche (Spain).

Figure 7: PVC attachment and plates used in the drift tests.

Figure 8: Experimental drop size distribution data.

Figure 9: Experimental cumulative drop mass distribution, Rosin–Rammler distribution, Modified Rosin–Rammler distribution and Log-normal distribution curves.

Figures

Fig_3a.eps

(a)

Fig_3b.eps

(b)

Fig_3c.eps

(c)

Fig_3d.eps

(d)

Figure 1: (a) Original image, (b) R-channel, (c) G- channel and (d) B-channel.

Fig_4a.eps

(a)

Fig_4b.eps

(b)

Figure 2: (a) Original image and (b) processed image.

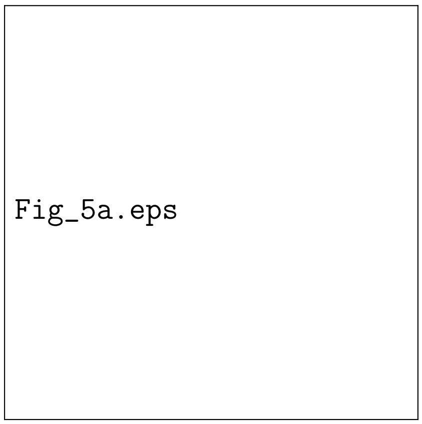

(a) (b)

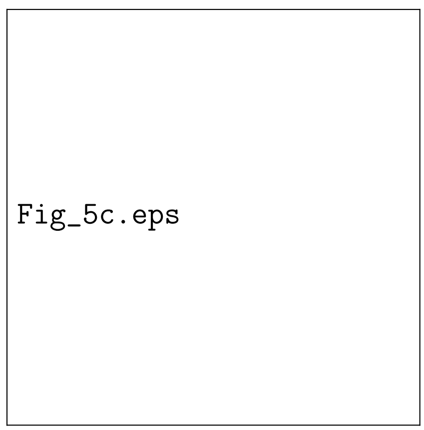

(c)

Figure 3: Data types for the stains detected. a) “No Drop”, b) “Drop” and c) “Multiple Drop”.

Fig_6.eps

Figure 4: Spread factor curve for Teejet 52 x 76 mm paper.

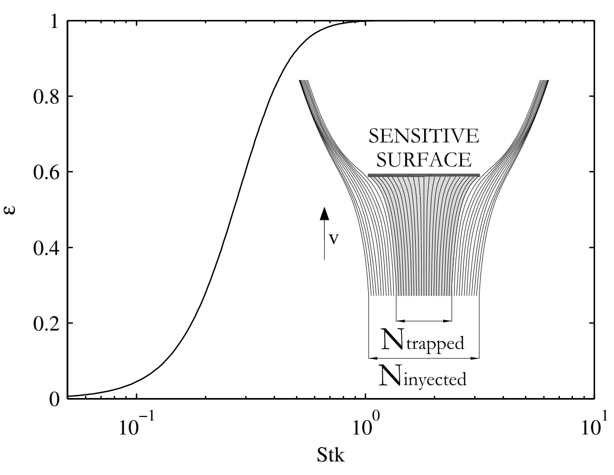

Figure 5: Experimental impaction efficiency of ribbons provided by May and Clifford (1967) and schematic arrangement of particle deposition on sensitive papers.

Fig_8.eps

Figure 6: Arragement of the pilot test facility assembled at Universidad Miguel Hernández, Elche (Spain).

Fig_9.eps

Figure 7: PVC attachment and plates used in the drift tests.

Fig_10a.eps

(a) Test run number 1

Fig_10b.eps

(b) Test run number 2

Fig_10c.eps

(c) Test run number 3

Fig_10d.eps

Fig_11a.eps

(a) Test run number 1

Fig_11b.eps

(b) Test run number 2

Fig_11c.eps

(c) Test run number 3

47

Fig_11d.eps